

# Local and Nonlocal Functions of Cs Promoter in the O<sub>2</sub>-Oxidation of Graphite

J. R. Hahn and H. Kang\*

School of Chemistry, Seoul National University, Kwanak-ku, Seoul, South Korea 151-742

Received: March 14, 2002

The O<sub>2</sub> oxidation reaction of graphite was studied by preparing Cs promoters in two different states: Cs adsorbed on a surface [Cs(ad)] and Cs trapped underneath a surface carbon plane [Cs(tr)]. Reactive ion scattering spectrometry (RIS) and scanning tunneling microscopy (STM) were used to identify the reaction intermediates and to measure the spatial range of the Cs promoter effect. Cs(ad) promotes the oxidation reaction in a localized region through formation of CsO and CsO<sub>2</sub> intermediates. On the other hand, Cs(tr) promotes the reaction over a long range, such that a large number ( $\sim 10^3$ ) of O<sub>2</sub> molecules are chemisorbed at a graphite surface and etch away the surface carbons.

## 1. Introduction

The reactivity of a solid surface is often dramatically changed by adsorption of electropositive or electronegative atoms. This phenomenon, known as the promotion or poisoning effect in heterogeneous catalysis, has been observed on various types of surfaces including metals,<sup>1–4</sup> semiconductors,<sup>5–7</sup> and semimetals such as graphite.<sup>8–12</sup> The oxidation of graphite by O<sub>2</sub> molecules is an example in which the alkali-metal promotion effect has been extensively studied.<sup>8–12</sup> The reaction has served as a model system to understand the technologically important processes such as coal gasification, combustion, and water-gas production, owing to the simplicity of the reaction scheme involving only a few oxidation products and a two-dimensional graphite lattice. Kasemo and co-workers<sup>9,10</sup> examined graphite oxidation in the presence of potassium promoters. They found that O<sub>2</sub> molecules are captured on a graphite surface in the form of KO<sub>2</sub> and K<sub>2</sub>O complexes, which then react with surface carbons to produce CO and CO<sub>2</sub> gas. The observation shows that the reaction is promoted by the direct interactions of potassium with O<sub>2</sub> through the so-called oxygen-transfer mechanism.<sup>13,14</sup> Alternatively, an indirect promotion mechanism has been suggested,<sup>14</sup> in which alkali metals transfer the charges to a surface, subsequently increasing the carbon–oxygen bond strength and reactivity of the surface. The indirect promotion by electron transfer has not yet found conclusive experimental evidence in graphite oxidation. Electron transfer is believed to be responsible for the promotion of many other types of surfaces as well.<sup>1–4,7,10,14</sup> It has been difficult, however, to separate experimentally the direct and the indirect functions of a promoter. The two functions might have different spatial ranges of influence, but the exact range is still a controversial issue on various surfaces.<sup>1–4,6,7,9,10,14,15</sup> Thus, to date, some important questions remain to be answered for the role of alkali-metal promoters, which may be phrased as follows: (1) What is the chemical identity of reaction intermediates? (2) Does a promoter react directly or indirectly with molecules? (3) What is the spatial range of the promoter effects?

We focused on these issues in the present study of O<sub>2</sub>-oxidation of graphite promoted by Cs. For systematic investigation of the promoter functions, two different states of Cs

promoters were prepared: Cs adsorbed on a surface [Cs(ad)] and Cs trapped beneath a graphite surface [Cs(tr)]. In the latter case, a carbon plane prohibits a direct contact between Cs and O<sub>2</sub>. The surface intermediates formed in the reactions were examined by Cs<sup>+</sup> reactive ion scattering spectrometry (Cs<sup>+</sup>-RIS). In this technique, a hyperthermal (10–100 eV) Cs<sup>+</sup> ion beam is scattered from a surface, and the scattered ions are mass-analyzed.<sup>16</sup> The scattered ions are composed of reflected primaries and RIS products which are association products of Cs<sup>+</sup> with molecules at the surface. The greatest advantage of the technique is the unambiguous identification of molecules on surfaces.<sup>16</sup> An STM operated in ultrahigh vacuum (UHV)<sup>17</sup> was used to examine the local density of states (LDOS) of a surface and the topographical changes resulting from the oxidation reaction.

## 2. Experimental Section

Highly ordered pyrolytic graphite samples (HOPG, Advanced Ceramics Co., ZYA grade) were cleaved with an adhesive tape in air and transferred to a UHV chamber. The samples were cleaned in UHV by degassing at 650 °C for several hours and flashing to 1000 °C for several minutes. Oxidation reaction of graphite was carried out in RIS<sup>16</sup> and STM<sup>17</sup> UHV chambers. In the RIS chamber with a base vacuum of  $2 \times 10^{-10}$  Torr, Cs(ad) and Cs(tr) were prepared on an (0001) surface of a sample by the impact of mass- and energy-selected Cs<sup>+</sup> ion beams (10–100 eV) at normal incidence. The beam dose was controlled to produce a small coverage (<1% of monolayer) of Cs on the surface at the current density of 0.1–10 nA/cm<sup>2</sup> and the beam exposure time of up to several minutes. The sample was then exposed to O<sub>2</sub> gas at a pressure of  $2 \times 10^{-7}$  Torr at room temperature. The species formed on the surface were identified by RIS measurement, in which the RIS product ions were analyzed for their mass by a quadrupole mass spectrometer operated in a positive-ion sampling mode. High-temperature oxidation reaction was studied in the STM chamber, in which a graphite sample with Cs(ad) or Cs(tr) was exposed to O<sub>2</sub> gas at  $2 \times 10^{-7}$  Torr and then heated to 560 °C in UHV. The surface was examined by STM before and after the oxidative etching experiment. The transfer of samples between RIS and STM chambers was done using a vacuum-transfer line pumped by a small ion pump.

\* Corresponding author. Fax: +82-2-889-8156. E-mail: surfion@snu.ac.kr.

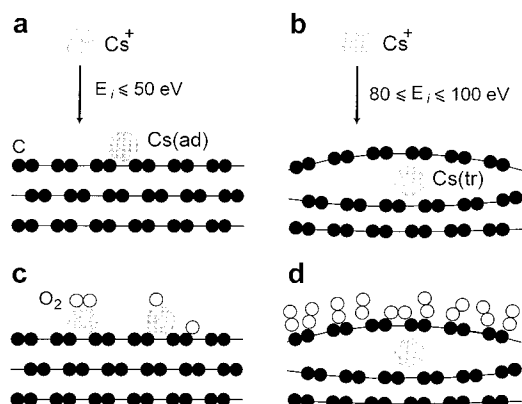


**Figure 1.** Cs promoters and the adsorption of oxygen on the promoted graphite surfaces. Cesium is drawn as a large gray circle, carbon as a small black circle, and oxygen as a white circle. The circle sizes are scaled to covalent atomic (C and O) and ionic (Cs<sup>+</sup>) radii. The diagram illustrates the formation of (a) Cs(ad) and (b) Cs(tr) by the impact of Cs<sup>+</sup> on graphite at a controlled beam energy. Adsorption of O<sub>2</sub> gas on these surfaces produces the reaction intermediates shown in (c) and (d). The detailed geometries of CsO, CsO<sub>2</sub>, and O<sub>2</sub> at the surfaces are arbitrarily drawn.

### 3. Results

We prepared a graphite sample which selectively contains either Cs(ad) or Cs(tr), by impinging a Cs<sup>+</sup> ion beam to the (0001) surface of graphite at a controlled energy. The methods for generating interstitial atoms by low-energy ion impact and their identification were described previously.<sup>17</sup> Following these procedures, we found that the threshold energy for Cs<sup>+</sup> penetration into a (0001) surface lies between 50 and 80 eV. Therefore, a Cs<sup>+</sup> beam at energy <50 eV was used to produce Cs(ad) and a beam at 80–100 eV to produce Cs(tr), as schematically illustrated in Figure 1a,b. At 80–100 eV, Cs<sup>+</sup> ions penetrate only to the first carbon layer, producing Cs(tr) trapped between the first and the second layers. The embedded depth of Cs(tr) was revealed by high-temperature etching of a graphite surface in O<sub>2</sub> gas and by imaging the etched surface with STM;<sup>18</sup> the STM images showed that the etched pits were all monolayer deep.

The Cs<sup>+</sup> impact at 80–100 eV produced carbon vacancies in addition to Cs(tr)'s by displacing surface carbon atoms permanently.<sup>17</sup> The populations of Cs(tr) and carbon vacancy were measured with STM, after separating the two defects according to the following procedure.<sup>17</sup> Cs(tr) was selectively removed from the sample by heating to 560 °C in a vacuum, a condition in which carbon vacancies are not destroyed. Cs(ad), if also existed on the surface, would desorb well below this temperature. The elimination of Cs(ad) and Cs(tr) was checked by Auger electron spectroscopy (AES) and Cs<sup>+</sup>-RIS. The defect populations were measured before and after the sample heating by STM imaging, which revealed that Cs(tr) consisted more than 90% of the total defects generated by 80–100 eV Cs<sup>+</sup> impact.

The samples containing Cs(ad) or Cs(tr), prepared as described above, were exposed to O<sub>2</sub> gas at a pressure of  $2 \times 10^{-7}$  Torr at room temperature, and then their surface was examined by Cs<sup>+</sup>-RIS. Figure 2a presents a Cs<sup>+</sup>-RIS spectrum obtained from a Cs(tr)/graphite surface reacted with O<sub>2</sub>. The energy of a Cs<sup>+</sup> probe beam was 20 eV. In the spectrum, the reflected Cs<sup>+</sup> appears as an intense peak at 133 amu/charge. Another peak at 165 amu/charge represents CsO<sub>2</sub><sup>+</sup>, formed by the pickup of O<sub>2</sub> species on the surface by scattered Cs<sup>+</sup> ions. The O<sub>2</sub> species must be bonded directly to a surface carbon

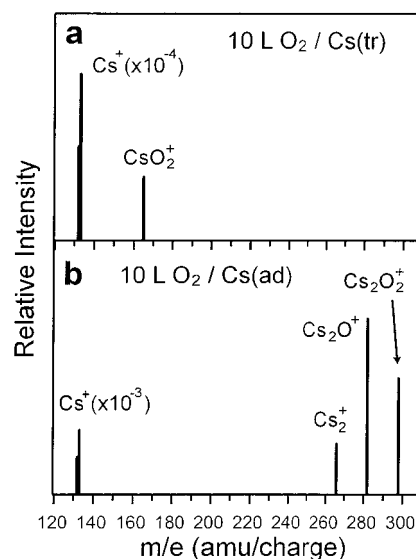


**Figure 2.** Cs<sup>+</sup>-RIS spectra obtained from graphite surfaces after O<sub>2</sub> adsorption at room temperature in the presence of Cs promoters. (a) 10 L of O<sub>2</sub> gas was exposed to a Cs(tr)/graphite surface, prepared by the impact of 100 eV Cs<sup>+</sup> ions at a current density of 7 nA/cm<sup>2</sup> for 3 min. (b) 10 L of O<sub>2</sub> was exposed to Cs(ad)/graphite formed by the deposition of a 15 eV Cs<sup>+</sup> beam at a current density of 7 nA/cm<sup>2</sup> for 3 min. RIS measurements were made with a Cs<sup>+</sup> probe beam of 20 eV in a 45°/45° specular scattering geometry. Intensity of the Cs<sup>+</sup> peak is reduced by the factors indicated. The RIS peaks in spectrum (a) indicate the presence of O<sub>2</sub>(ad), and in spectrum (b), Cs(ad), CsO(ad), and CsO<sub>2</sub>(ad).

plane, since there was no Cs(ad) on the surface (note that the Cs<sub>2</sub><sup>+</sup> signal at 266 amu/charge is absent). Figure 2b shows the result of O<sub>2</sub> adsorption on a Cs(ad)/graphite surface. Three RIS peaks appear in the spectrum, Cs<sub>2</sub><sup>+</sup> (266), Cs<sub>2</sub>O<sup>+</sup> (282), and Cs<sub>2</sub>O<sub>2</sub><sup>+</sup> (298 amu/charge), which are due to the pickup of Cs, CsO, and CsO<sub>2</sub>, respectively, from the surface. Higher cluster species (>300 amu/charge) were not able to be measured because the mass spectrometer had a limited mass range. The three signals indicate that O<sub>2</sub> reacts directly with Cs(ad) to form CsO(ad) and CsO<sub>2</sub>(ad). Note that the CsO<sub>2</sub><sup>+</sup> peak due to a chemisorbed O<sub>2</sub> molecule was not observed on this surface. A mass spectrum in the lower mass region (<133 amu/charge, not shown) revealed the presence of H<sup>+</sup> and other alkali-metal ions at impurity levels, but no oxygen-related peaks were observed.

We imaged the Cs-containing graphite surfaces with STM. Cs(tr) appeared as a protrusion in STM image, with its height mostly <10 Å and diameter <60 Å, in agreement with a previous report.<sup>19</sup> The protrusion has been attributed to an increase of LDOS at the graphite surface by charge transfer from Cs(tr) and/or geometric elevation of the surface plane in the presence of Cs(tr).<sup>17,20</sup> Cs(ad) was not able to be imaged by STM, reflecting a mobile nature of Cs(ad) on graphite during an STM scan at room temperature. These STM features were not changed noticeably after room-temperature adsorption of O<sub>2</sub> on the surfaces.

Following O<sub>2</sub> adsorption at room temperature, the samples were heated to 560 °C in a vacuum to induce oxidation reactions, and the resulting surfaces were examined by STM. Figure 3a presents an STM image obtained after heating an O<sub>2</sub>/Cs(ad)/graphite surface. The image is characterized by bright spots (protrusions) randomly dispersed on the surface, which were absent from the surface before the heating. Most of the bright spots are smaller than 30 Å in diameter and lower than 10 Å in height. The bright spots are interpreted to be carbon vacancies

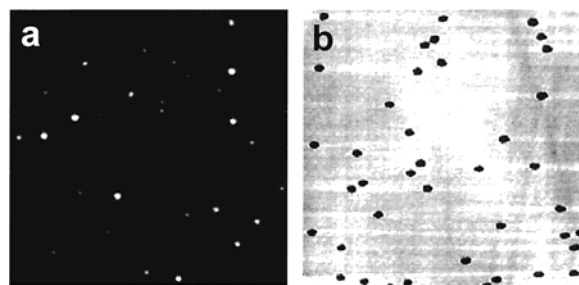


**Figure 3.** STM topographical images of graphite surfaces obtained after O<sub>2</sub> adsorption in the presence of Cs promoters followed by heating at 560 °C. (a) Exposure of 10 L of O<sub>2</sub> gas on Cs(ad)/graphite prepared from a 15 eV Cs<sup>+</sup> beam. The scan area is 110 nm × 110 nm. (b) Exposure of 10 L of O<sub>2</sub> on Cs(tr)/graphite prepared by Cs<sup>+</sup> impact at 100 eV. The scan area is 150 nm × 150 nm. The bright spots in image (a) are due to graphite vacancies, and the dark holes in image (b) are monolayer-etched pits (see text). The images were obtained at a sample bias of 100 mV and a tunneling current of 0.5 nA.

at the surface, which are produced by O<sub>2</sub>-etching of surface carbons at high temperature. Note that Cs(ad) was desorbed from the surface by heating. According to theoretical and experimental reports,<sup>17,18,21–23</sup> a graphite vacancy increases an LDOS near the Fermi level and thus is imaged as a protrusion by STM. The LDOS enhancement effect is profound only when the size of a vacancy is very small.<sup>17,22</sup> In other words, when a vacancy is etched further by O<sub>2</sub> reactions such that it forms a large-sized pit, the protrusion in STM image is changed to a dip.<sup>18</sup> Therefore, the bright spots in Figure 3a are considered to represent the vacancy structures of one to several missing atoms.

Figure 3b presents an STM topographical image from an O<sub>2</sub>/Cs(tr)/graphite surface heated to 560 °C. The image shows that the heating produced pits on this surface, in contrast to the formation of atomic vacancies from Cs(ad). The pits are substantially large in size (65 Å in average diameter), approximately circular, and have a monolayer depth (3.35 Å). These features are characteristic of an O<sub>2</sub>-etched graphite surface.<sup>18</sup> Since there was no extra oxygen supply inside the vacuum chamber during the heating, the etching must have occurred by reactions with O<sub>2</sub> molecules chemisorbed at the surface, revealed by the CsO<sub>2</sub><sup>+</sup> RIS signal (Figure 2a). Carbon vacancy, which exists on the surface in a small population, cannot be oxidized to such a large pit just by heating in a vacuum; a continuous supply of O<sub>2</sub> gas is needed to etch the vacancy.<sup>18</sup> The average pit area indicates the etching removes about 1 × 10<sup>3</sup> surface carbon atoms per pit. Considering that the O<sub>2</sub>-etching reaction is stoichiometric, producing CO or CO<sub>2</sub> gas,<sup>18,24,25</sup> the number of O<sub>2</sub> molecules that are chemisorbed at the surface should be similar [(0.5–1) × 10<sup>3</sup> O<sub>2</sub> molecules per Cs(tr)]. We observed that the pit size was increased mildly by increasing the O<sub>2</sub> gas exposure, reaching a diameter of 100 Å when 80 L of O<sub>2</sub> was exposed on the surface.

We performed control experiments of O<sub>2</sub> oxidation on graphite surfaces containing Ar(tr) and Kr(tr). These noble gas interstitials were generated by impinging Ar<sup>+</sup> and Kr<sup>+</sup> beams at energies slightly above their surface penetration threshold, which is 38 eV for Ar<sup>+</sup> and 41 eV for Kr<sup>+</sup>.<sup>17</sup> The interstitial formation was verified by STM.<sup>17</sup> In contrast to Cs(tr), the noble gas atoms did not induce pit formation by the same oxidation procedure. The result reveals that the pit formation is not related to the ion-induced damages at a graphite plane, such as vacancy defects and other possible reactive sites formed by geometric disordering of surface carbons upon ion impact. Experiment with Xe(tr) was unsuccessful, because Xe<sup>+</sup> beams extensively

damaged a graphite surface rather than cleanly generated Xe(tr), due to a substantially larger size of a Xe<sup>+</sup> projectile than the others.

#### 4. Discussion

The experimental results show that the O<sub>2</sub>-etching behavior is clearly different depending on whether Cs(ad) or Cs(tr) is present on graphite. In the following, we explain the observed differences in the light of the precursor species identified by Cs<sup>+</sup>-RIS (Figure 2). On a Cs(ad)/graphite surface, O<sub>2</sub> molecules are adsorbed to the surface such that they bind to Cs(ad) and form CsO<sub>2</sub>(ad) and CsO(ad). The CsO(ad) formation involves O<sub>2</sub> dissociation and production of an extra O atom, which may be attached to another Cs(ad) or to nearby surface carbons. These precursor species are pictorially illustrated in Figure 1c. Cs(ad) can facilitate O<sub>2</sub> dissociation by charge donation from Cs(ad) to fill the 1π<sub>g</sub> orbital of O<sub>2</sub>.<sup>12</sup> The detection of CsO<sub>2</sub>(ad) and CsO(ad) parallels the previous observation of KO<sub>2</sub>(ad) and K<sub>2</sub>O(ad) in the K-promoted O<sub>2</sub>-oxidation of graphite.<sup>9</sup> At elevated temperature, O<sub>2</sub> and O in these precursors react off carbon atoms as CO or CO<sub>2</sub> gas. This stoichiometric reaction will remove one or at most a few surface carbons in the vicinity of Cs(ad) due to a limited available source of oxygen, leading to formation of a carbon vacancy.

On a Cs(tr)/graphite surface, O<sub>2</sub> exposure at room temperature leads to chemisorption of O<sub>2</sub> molecules at the surface carbon plane. The nature of chemisorbed O<sub>2</sub> must be quite different from physisorbed O<sub>2</sub>, since the former readily dissociates at a high temperature to react with surface carbons. Two possible reasons may be considered for why O<sub>2</sub> chemisorption is promoted by Cs(tr). First, Cs(tr) donates its charge to surface carbons to increase the LDOS of the surface, and consequently the surface reactivity toward O<sub>2</sub>. The charge transfer from Cs to a graphite plane has been well-known in intercalated systems.<sup>26,27</sup> Second, a surface carbon plane can be deformed upward by the presence of interstitial atoms.<sup>20</sup> This geometric deformation can increase the LDOS of surface carbons near the Fermi level. The LDOS change occurs as a result of the distorted interaction within the sp<sup>2</sup> band in the surface layer or the electronic disturbance in p<sub>z</sub>-p<sub>z</sub> overlap between the basal planes.<sup>17</sup> To estimate the degree of geometric deformation, we compare the diameter of the interstitial atoms employed in this study: 3.8 Å (Ar), 4.1 Å (Kr), 4.5 Å (Cs), and 3.7 Å (Cs<sup>+</sup>). Since Cs(tr) will carry a partial positive charge inside a graphite lattice as for Cs intercalants (Cs<sup>δ+</sup> with δ = 0.6–0.9 for the intercalants),<sup>26,27</sup> the diameter of Cs(tr) will be between 3.7 and 4.5 Å. This comparison suggests that Cs(tr) will cause a geometric deformation to a degree similar to Ar(tr) and Kr(tr), at least not far greater than them. These considerations lead us to interpret that the promoted O<sub>2</sub> chemisorption is primarily due to the charge-donating effect of Cs(tr), whereas the geometric deformation of a carbon surface has a relatively insignificant effect.

An important feature of Cs(tr) promotion is that Cs(tr) is able to hold an enormously large number (~10<sup>3</sup>) of O<sub>2</sub> molecules at the surface. The quantitative estimation for the number of chemisorbed O<sub>2</sub> molecules is deduced from the etching yield of surface carbons measured by STM. We can check if this estimation is consistent with other measurements. The RIS yield for chemisorbed O<sub>2</sub> species is about 4 × 10<sup>-5</sup> in Figure 2a (the intensity ratio of CsO<sub>2</sub><sup>+</sup> and Cs<sup>+</sup> peaks). To compare, a similar magnitude of RIS yield was observed for CO chemisorbed on Ni(111) at 0.5 monolayer coverage (1.0 × 10<sup>15</sup> CO molecules/cm<sup>2</sup>).<sup>16b</sup> If we assume that RIS detection efficiencies are similar



for O<sub>2</sub> and CO since they have similar masses and both are nonpolar diatomic molecules, we can deduce a surface density of  $1.0 \times 10^{15}$  O<sub>2</sub> molecules/cm<sup>2</sup> in Figure 2a. Cs(tr) has a number density of about  $4 \times 10^{11}$ /cm<sup>2</sup> on this surface as calculated from the given Cs<sup>+</sup> beam dosage and the Cs(tr) formation efficiency of 0.05 per ion impact at 100 eV.<sup>17</sup> The number density of Cs(tr) estimated in this way is consistent with the density of pits appeared in STM image (Figure 3b). With these numbers, we obtain that  $2.5 \times 10^3$  O<sub>2</sub> molecules are chemisorbed per Cs(tr), which is in reasonable agreement with the result from the carbon etching yield. One might question why the RIS yield is higher for Cs, CsO, and CsO<sub>2</sub> than for O<sub>2</sub> in Figure 2. The high RIS sensitivity for these Cs-containing species can be rationalized in terms of their very strong binding forces to a Cs<sup>+</sup> projectile.<sup>16</sup> AES analysis has been reported<sup>19</sup> for O<sub>2</sub> adsorption on a Cs(tr)/graphite surface prepared by 80 eV Cs<sup>+</sup> impact. The AES spectrum shows that the amount of oxygen on the surface is substantially large, although its quantification was not performed.

As mentioned in Section (1), two mechanisms have been suggested for the functions of alkali-metal promoters in graphite oxidation. In the oxygen-transfer mechanism, a promoter enhances the oxidation rate by directly reacting with O<sub>2</sub> and forming reaction intermediates.<sup>9,10,13,14</sup> The observation of CsO-(ad) and CsO<sub>2</sub>(ad) precursors verifies that Cs(ad) promotes the reaction through this mechanism. We also found that Cs(ad) promotes the reaction in a very localized manner, resulting in the etching of a few carbon atoms at most and the production of atomic vacancies. Another suggested mechanism is the indirect electron transfer from a promoter to O<sub>2</sub> through a carbon plane. The enhanced graphite etching by Cs(tr) is a clear experimental evidence of this mechanism observed for the first time. The reaction intermediate in this case is O<sub>2</sub> species bonded directly to a carbon surface. Importantly, Cs(tr) promotes the surface reactivity over a long range, such that a large number of O<sub>2</sub> molecules are chemisorbed and react off carbon atoms in a promoted region.

## 5. Conclusions

We have provided direct evidence for the promotion mechanisms of Cs in the graphite oxidation reaction, by identifying CsO and CsO<sub>2</sub> as the intermediates in the oxygen-transfer mechanism, and chemisorbed O<sub>2</sub> in the electron-transfer mechanism. The spatial range of the promoter function is very different for the two mechanisms. The charge transfer from Cs-(tr) to O<sub>2</sub> through a graphite layer promotes the O<sub>2</sub> reactivity over a long range, resulting in a carbon etching yield in the order of 10<sup>3</sup> atoms per Cs(tr), whereas the promotion via Cs-(ad)-oxygen complex formation produces a very localized effect. We must recognize, however, that the high etching yield due to the electronic promotion does not mean that this mechanism will always prevail in graphite oxidation processes taking place in other conditions, since the present reaction condition is rather unique. Nevertheless, the result shows that the electronic promotion can occur, and when it does, it gives an overwhelming effect on the etching yield. It can easily be

imagined that such electronic promotion will be important not only for graphite, but also for other surfaces on which the extra charge donated from an alkali-metal promoter can be spread out.

**Acknowledgment.** We thank S.-C. Park and K.-Y. Kim for many useful discussions. This work was supported by the BK21 Program of the Ministry of Education of Korea and by the SNU Development Fund.

## References and Notes

- (1) (a) Bonzel, H. P.; Bradshaw, A. M.; Ertl, G. *Physics and Chemistry of Alkali Metal Adsorption*, Material Science Monographs, Vol. 57; Elsevier: New York, 1989. (b) Pirug, G.; Bonzel, H. P. In *Structure of electrified interfaces*; Lipkowski, J., Ross, P. N., Eds.; VCH: New York, 1993; p 153.
- (2) Nørskov, J. K.; Holloway, S.; Lang, N. D. *Surf. Sci.* **1984**, *137*, 65.
- (3) (a) Markert, K.; Wandelt, K. *Surf. Sci.* **1985**, *157*, 24. (b) Feibelman, P. J.; Hamann, D. R. *Surf. Sci.* **1985**, *149*, 48.
- (4) (a) Bonzel, H. P. *Surf. Sci. Rep.* **1987**, *8*, 43. (b) Bonzel, H. P. *J. Vac. Sci. Technol. A* **1984**, *2*, 866.
- (5) (a) Faraci, G.; Pennisi, A. R.; Margaritondo, G. *Phys. Rev. B* **1996**, *53*, 13851. (b) Saukiassian, P.; Bakashi, M. H.; Starnberg, H. I.; Hurych, G.; Gentle, T. M.; Chuette, K. P. *Phys. Rev. Lett.* **1987**, *13*, 1488.
- (6) (a) Masscaraque, A.; Ottaviani, C.; Capozzi, M.; Pedio, M.; Michel, E. G. *Surf. Sci.* **1997**, *377*, 650. (b) Ernst, H.-J.; Yu, M. L. *Phys. Rev. B* **1990**, *41*, 12953.
- (7) (a) Gorelik, D.; Aloni, S.; Eitle, J.; Meyler, D.; Haase, G. *J. Chem. Phys.* **1998**, *108*, 9877. (b) Starnberg, H. I.; Saukiassian, P.; Hurych, Z. *Phys. Rev. B* **1989**, *39*, 12775.
- (8) Hock, K. M.; Barnard, J. C.; Palmer, R. E.; Ishida, H. *Phys. Rev. Lett.* **1993**, *71*, 641.
- (9) (a) Sjöval, P.; Kasemo, B. *J. Chem. Phys.* **1993**, *98*, 5932. (b) Chakarov, D. V.; Sjöval, P.; Kasemo, B. *J. Phys. Condens. Matter* **1993**, *5*, 2903. (c) Janiak, C.; Hoffmann, R.; Sjöval, P.; Kasemo, B. *Langmuir* **1993**, *9*, 3427.
- (10) Sjöval, P.; Hellsing, B.; Keck, K.-E.; Kasemo, B. *J. Vac. Sci. Technol. A* **1987**, *5*, 1065.
- (11) Sandell, A.; Hjortstam, O.; Nilsson, A.; Brühwiler, P. A.; Eriksson, O.; Bennich, P.; Rudolf, P.; Wills, J. M.; Johansson, B.; Mårtensson, N. *Phys. Rev. Lett.* **1997**, *78*, 4994.
- (12) Lamoén, D.; Persson, B. N. J. *J. Chem. Phys.* **1998**, *108*, 3332.
- (13) Wood, B. J.; Sancier, K. M. *Catal. Rev. Sci. Eng.* **1984**, *26*, 233.
- (14) (a) McKee, D. W. In *Chemistry and Physics of Carbon*, Vol. 16; Marcel Dekker: New York, 1981; p 1. (b) McKee, D. W. *Fuel* **1983**, *62*, 170.
- (15) Albano, E. V. *Surf. Sci.* **1989**, *215*, 333.
- (16) (a) Yang, M. C.; Hwang, C. H.; Kang, H. *J. Chem. Phys.* **1997**, *107*, 2611. (b) Kang, H.; Kim, K. D.; Kim, K. Y. *J. Am. Chem. Soc.* **1997**, *119*, 12002.
- (17) Hahn, J. R.; Kang, H. *Phys. Rev. B* **1999**, *60*, 6007.
- (18) (a) Lee, S. M.; Lee, Y. H.; Hwang, Y. G.; Hahn, J. R.; Kang, H. *Phys. Rev. Lett.* **1999**, *82*, 217. (b) Hahn, J. R.; Kang, H.; Lee, S. M.; Lee, Y. H. *J. Phys. Chem. B* **1999**, *103*, 9944.
- (19) Hahn, J. R. *Surf. Sci.* **1999**, *423*, L216.
- (20) Marton, D.; Bu, H.; Boyd, K. J.; Todorov, S. S.; Al-Bayati, A. H.; Rabalais, J. W. *Surf. Sci.* **1995**, *326*, L489.
- (21) Hahn, J. R.; Kang, H.; Song, S.; Jeon, I. C. *Phys. Rev. B* **1996**, *53*, R1725.
- (22) Lee, K. H.; Lee, H. N.; Eun, H. M.; Lee, W. R.; Kim, S.; Kim, D. *Surf. Sci.* **1994**, *321*, 267.
- (23) Nordlund, K.; Keinonen, J. *Phys. Rev. Lett.* **1996**, *77*, 699.
- (24) Yang, R. T. In *Chemistry and Physics of Carbon*, Vol. 19; Marcel Dekker: New York, 1984; p 163.
- (25) Yang, Y. W.; Hrbek, J. *J. Phys. Chem.* **1995**, *99*, 3229.
- (26) Dunlap, B. I.; Ramaker, D. E.; Murday, J. S. *Phys. Rev. B* **1982**, *25*, 6439.
- (27) Whangbo, M.-H.; Liang, W.; Ren, J.; Magonov, S. N. *J. Phys. Chem. B* **1994**, *98*, 7602.